Annals of Biomedical Engineering, Vol. 16, pp. 445-461, 1988
Printed in the USA.

0090-6964/88 $3.00 + .00

CO_2 CONTROL OF THE RESPIRATORY SYSTEM: PLANT DYNAMICS AND STABILITY ANALYSIS

Ahmed ElHefnawy,* Gerald M. Saidel, Eugene N. Bruce

Department of Biomedical Engineering
Case Western Reserve University
Cleveland, OH 44106

(Revised 1/5/88)

A stability analysis of respiratory chemical control is developed using a mathematical model of CO_2 mass transport dynamics. Starting with a 3-compartment model of CO_2 stores that distinguishes alveolar, muscle, and other tissue, model reduction techniques are applied to obtain a first-order representation of the respiratory plant. This model contains an effective tissue volume for CO_2, whose derived value is much smaller than previously predicted. To investigate oscillatory instabilities, a controller which incorporates only peripheral chemoreceptor responses was added to the first-order plant model. An explicit stability index (SI) is obtained analytically from a linearized version of this model. SI varies directly with the controller gain and circulation delay time and inversely with the effective tissue volume and inspired CO_2 concentration. Numerical simulations using the first-order nonlinear model show that SI is a good predictor of system stability. According to the linearized model, the system is stable for $SI < 1$; from the nonlinear model, the system is stable for $SI < 1.1$. For typical normal adults, the SI value is well within the stable region.

Keywords—*Periodic breathing, Respiratory control, Mathematical model, CO_2 mass transport, Stability.*

INTRODUCTION

Short-term periodicities (STP) are cyclic changes in ventilation and composition of respiratory gases having periods ranging from 20 to 120 seconds. Such periodicities have been reported under various pathological, nonpathological, and experimental conditions. Numerous mechanisms underlying STP have been proposed from theoretical (9,13,14,15,16,17,18,19), physiological (6,11), and clinical studies (3,4,8). These mechanisms can be grouped into two categories. The first is based on the hypothesis that the causes of STP are the dynamic interactions among the various chemical and/or mechanical feedback loops of the respiratory control system (5). Alternatively, STP may arise from oscillations in the neural circuits of the respira-

Acknowledgment—Supported in part by a grant from NIH (HL-25830).

*Ahmed ElHefnawy is supported in part by a fellowship from the Egyptian Ministry of Higher Education; he is currently on leave of absence from Cairo University.

Address correspondence to Gerald M. Saidel, Department of Biomedical Engineering, Case Western Reserve University, Cleveland, OH 44106.

tory centers independently from the feedback control (26). Within these categories, investigators have considered neurological (2,21), cardiovascular (22,23), and/or mechanical factors (24) that may account for manifestations of STP.

The work presented in this paper is a systematic investigation of the hypothesis that the stability characteristics associated with CO_2 control of the respiratory system determine STP. Although this hypothesis was examined by Milhorn *et al.* (19) using model simulations, they did not develop an analytical stability criterion by which to understand how combinations of parameters would affect the stability of ventilation. Furthermore, many of their model predictions of unstable conditions are outside the physiological range (2). An implicit stability criterion was developed by Khoo *et al.* (13), but simulations of the system dynamics and output sensitivity to parameter values were not investigated. The explicit criterion developed by Glass and Mackey (9) and Mackey *et al.* (16) has limited physiological significance because the parameters were based on an empirical model of CO_2 plant dynamics.

The above limitations have been addressed in the current study using both analytical and simulation techniques. We show that unstable behavior of the system is a likely underlying mechanism of STP behavior. Starting with mass balance equations of CO_2 dynamics for a respiratory plant comprising several tissue compartments, we rigorously develop a simplified model of the plant. The parameters of this simple first-order plant model are directly related to physiological parameters of the more general model. To study stability, we assume a time-delay relation for the feedback control of ventilation. Following Khoo *et al.* (13) we assume that the contribution of central chemosensory mechanisms to STP is negligible. Accordingly, the controller represents only the dependence of ventilation on peripheral chemoreceptor input. Finally, using the analytic technique of Hayes (12), an explicit criterion for predicting the occurrence of STP is derived which maps the relevant system parameters (e.g., tissue volume, controller gain and threshold, circulation delay, inspired CO_2 concentration) into a unified index of ventilatory stability.

MODELS OF CO_2 PLANT DYNAMICS

Three-Compartment Model

We shall consider a model of CO_2 dynamic mass balances for three perfectly mixed tissue compartments: alveolar (A), muscle (m), and other tissue (ot) as shown in Fig. 1. Within each compartment, CO_2 is assumed to be in chemical equilibrium. For the alveolar compartment, this implies that the CO_2 partial pressures of the alveolar gas (P_A) and of the arterial blood (P_a) are equal. The mass balance for alveolar CO_2 (in the Appendix) leads to the following alveolar partial pressure dynamics:

$$V_A dP_A/dt = \dot{V}_A(P_I - P_A) + \lambda Q[P_v^* - P_a] \tag{1}$$

where P_I is the inspired CO_2 partial pressure and $P_v^* = P_v(t - t_v)$ is the mixed-venous partial pressure with systemic venous delay time, t_v. Also, V_A is an equivalent volume for alveolar gas and tissue; $\dot{V}_A$ is the alveolar ventilation; Q is the pulmonary blood flow (assumed to equal cardiac output); λ is the CO_2 tissue-gas partition coefficient.

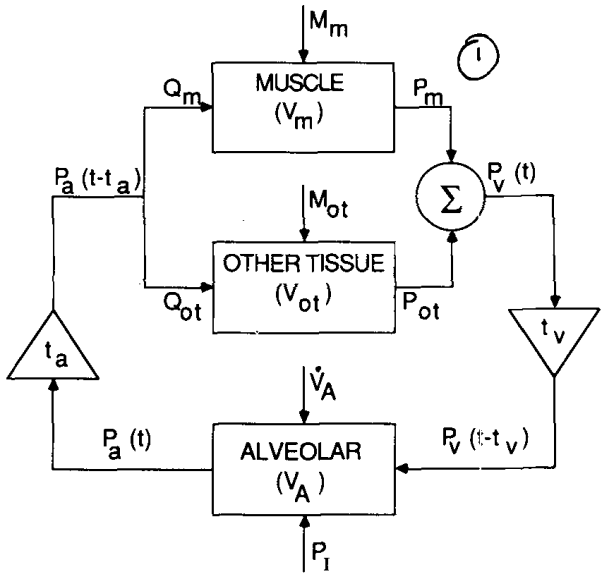

FIGURE 1. Schematic structure of the 3-compartment model described by Eqs. 1, 2, and 3.

In the resting state, the systemic tissues are distinguished as the (poorly perfused) muscle tissue and (well-perfused) other tissue. For the muscle compartment, the CO_2 mass balance (in the Appendix) can be expressed in terms of CO_2 partial pressure (P_m):

$$V_m dP_m/dt = M_m/k + Q_m[P_a^* - P_m] \tag{2}$$

where V_m is the muscle volume; M_m is the metabolic rate; Q_m is the muscle blood flow; and $P_a^* = P_a\ (t - t_a)$ where t_a is the systemic arterial delay time. The parameter k is the slope of the CO_2 equilibrium relation between total and free CO_2 in blood, muscle, and other tissue. As shown in the Appendix, $k = \lambda/RT$, where R is the ideal gas constant and T is the absolute temperature. A dynamic equation similar to Eq. 2 governs the CO_2 partial pressure of other tissue (P_{ot}):

$$V_{ot} dP_{ot}/dt = M_{ot}/k + Q_{ot}[P_a^* - P_{ot}]. \tag{3}$$

The parallel compartment outputs are the total blood flow

$$Q = Q_m + Q_{ot} \tag{4}$$

and the CO_2 partial pressure of the mixed venous blood:

$$P_v = [Q_{ot}P_{ot} + Q_m P_m]/Q. \tag{5}$$

Equations 1–5 will be referred to as the 3-compartment plant model (M3).

Equivalent Systemic Tissue Compartment

Let us consider how the two systemic tissue compartments can be combined into a single equivalent compartment described by an effective tissue CO_2 pressure (P_{tis}) which satisfies a dynamic relationship like that of each individual compartment:

$$V_{tis}\,dP_{tis}/dt = M_{tis}/k + Q[P_a^* - P_{tis}]. \tag{6}$$

We must relate M_{tis} and V_{tis} to the parameters of the two systemic tissue compartments. First, we see that the output of this compartment, P_{tis}, equals the summed outputs of the two systemic tissue compartments, P_v, as determined by Eq. 5:

$$P_{tis} = P_v = [Q_{ot}P_{ot} + Q_mP_m]/Q. \tag{7}$$

If the steady-state values for P_{tis}, P_m, P_{ot} (obtained by setting Eqs. 2, 3 and 6 equal to zero) are substituted into Eq. 7, then the metabolic rates can be related as:

$$M_{tis} = M_m + M_{ot}. \tag{8}$$

We now proceed to determine the effective tissue volume, V_{tis}, based on the effective tissue time constant:

$$\tau_{tis} = V_{tis}/Q. \tag{9}$$

This can be accomplished by examining the Laplace transform of Eq. 7:

$$\bar{P}_{tis}(s) = [Q_{ot}\bar{P}_{ot}(s) + Q_m\bar{P}_m(s)]/Q.$$

Substituting the solution for $\bar{P}_{ot}(s)$ from Eqs. 2 and 3, we obtain

$$\begin{aligned}\bar{P}_{tis}(s) \simeq \{&Q_m[M_m/sk + Q_m\bar{P}_a^*]/[sV_m + Q_m] \\ &+ Q_{ot}[M_{ot}/sk + Q_{ot}\bar{P}_a^*]/[sV_{ot} + Q_{ot}]\}/Q.\end{aligned} \tag{10}$$

For large s (or small t), Eq. 10 can be simplified to

$$\bar{P}_{tis}(s) \simeq [Q_m^2/V_m + Q_{ot}^2/V_{ot}]\bar{P}_a^*/sQ = \bar{P}_a^*/s\tau_{tis}$$

from which we get

$$\tau_{tis} = V_{tis}/Q = Q/[Q_m^2/V_m + Q_{ot}^2/V_{ot}]. \tag{11}$$

This result can be shown also by a time-domain perturbation analysis about the steady-state operating point. Consequently, we multiply Eq. 11 by Q to obtain

$$V_{tis} = Q\tau_{tis} = Q^2/[Q_m^2/V_m + Q_{ot}^2/V_{ot}]. \tag{12}$$

We can specify a reduced model (M2) consisting of the alveolar tissue and the equivalent systemic tissue compartment (Fig. 2). This M2 model can be restated from Eq. 1 (with $P^*_{tis} = P^*_v$) as

$$dP_A/dt = [P_I - P_A]/\tau_A + [P^*_{tis} - P_A]/\tau_e \tag{13}$$

and from Eq. 6 (with $P^*_A = P^*_a$) as

$$dP_{tis}/dt = M_{tis}/kQ\tau_{tis} + [P^*_A - P_{tis}]/\tau_{tis} \tag{14}$$

where we introduced the alveolar time constant

$$\tau_A = V_A/\dot{V}_A$$

and the exchange time constant

$$\tau_e = V_A/\lambda Q.$$

First-Order Plant Model

The plant model can be further reduced to a first-order system when the time delays within the plant are negligible with respect to other system time constants so that $P^*_{tis} = P_{tis}$ and $P^*_A = P_A$. Consequently, Eqs. 13 and 14 can be combined to form the following second-order system:

$$\begin{aligned}\tau_{tis} d^2P_{tis}/dt^2 + [1 + \tau_{tis}/\tau_A + \tau_{tis}/\tau_e]\, dP_{tis}/dt \\ = [P_I - P_{tis}]/\tau_A + [M_{tis}/kQ][1/\tau_A + 1/\tau_e].\end{aligned} \tag{15}$$

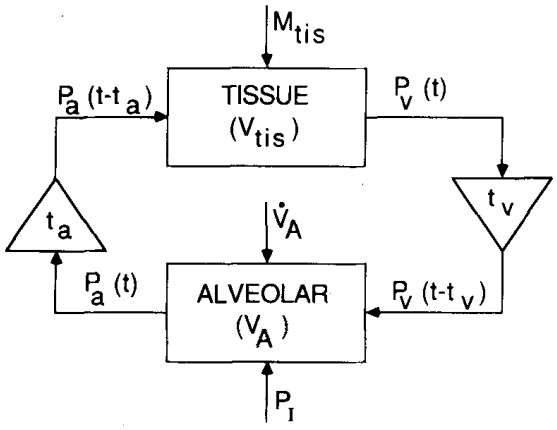

FIGURE 2. Schematic structure of the 2-compartment model described by Eqs. 13 and 14.

To determine the condition under which the second-order term can be neglected, we express the left-hand side of Eq. 15 in terms of dimensionless time, $\theta = t/\tau_{\text{tis}}$ which leads to

$$\{d^2P_{\text{tis}}/d\theta^2 + [1 + \tau_{\text{tis}}(1/\tau_A + 1/\tau_e)]\,dP_{\text{tis}}/d\theta\}/\tau_{\text{tis}}.$$

For typical human adult values (Table 1), the time constants satisfy the following inequality:

$$\tau_{\text{tis}}[1/\tau_A + 1/\tau_e] \gg 1.$$

From this inequality, Eq. 15 simplifies to a first-order system that approximates the CO_2 partial pressure of the system, $P_s \simeq P_{\text{tis}}$, according to

$$\tau_{\text{tis}}[1/\tau_A + 1/\tau_e]\,dP_s/dt = [P_I - P_s]/\tau_A + [1/\tau_A + 1/\tau_e]M_{\text{tis}}/kQ. \tag{16}$$

Furthermore, if

$$1/\tau_A \ll 1/\tau_e \Rightarrow \dot{V}_A/\lambda Q \ll 1$$

TABLE 1. Parameter values typical of normal, adult humans.[a]

G:	Effective CO_2 controller gain	2.33 L/min-mmHg
I:	Effective CO_2 controller intercept	96.0 L/min
k:	CO_2 equilibrium coefficient	0.167 mM/L-mmHg
M_m:	Muscle metabolic rate	1.49 mM/min
M_{ot}:	Other tissue metabolic rate	8.84 mM/min
[b]M_s:	Effective tissue metabolic rate	10.33 mM/min
[b]P_{so}:	Steady state CO_2 partial pressure	43.5 mmHg
[b]Q:	Cardiac output	5.9 L/min
Q_m:	Muscle blood flow	0.8 L/min
Q_{ot}:	Other tissue blood flow	5.1 L/min
R:	Universal gas content	62.37 L-mmHg/mole-°K
T:	Body temperature	310°K
t_d:	Plant-controller circulation delay	0.167 min
V_A:	Alveolar gas-tissue volume	3.5 L
V_m:	Muscle volume	29.1 L
V_{ot}:	Other tissue volume	9.6 L
[b]V_s:	Effective tissue volume	13.4 L
λ:	CO_2 blood-gas partition coefficient	3.23
[b]τ_{tis}:	Effective tissue time constant	2.3 min
[b]τ_A:	Alveolar time constant	0.7 min
[b]τ_e:	Exchange time constant	0.175 min

[a]Several of these parameters such as k, λ, and Q are dependent on the PCO_2 level.
[b]These parameters are derived from the other parameters according to the relationships given in the text.

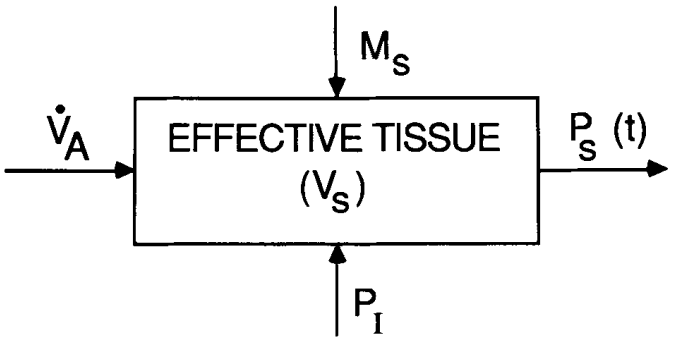

FIGURE 3. Schematic structure of the 1-compartment model described by Eq. 17.

then Eq. 16 becomes

$$dP_s/dt = [\dot{V}_A/\lambda V_S][P_I - P_s] + M_s/kV_s \tag{17}$$

where $V_s = V_{tis}$ and $M_s = M_{tis}$. From this first-order model (M1) of CO_2 respiratory dynamics (Fig. 3), a stability analysis can be made of the respiratory control system. Justification for using this reduced model in the stability analysis can be made by comparison of the M3, M2 and M1 models. Simulated responses of these models to a step input of 5% CO_2 applied at $t = 0$ are shown in Fig. 4. (The parameter values for these simulations are listed in Table 1.) The change of CO_2 partial pressure from its equilibrium level increases exponentially with time at a rate determined by the time

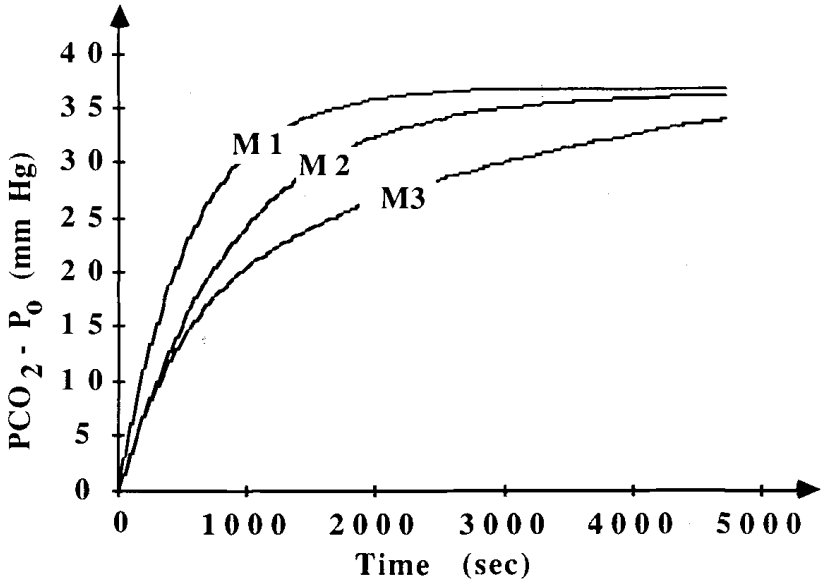

FIGURE 4. Open-loop step responses of plant model M1, M2, and M3, whose output (PCO_2) corresponds to P_s, P_v, and P_v, respectively, as shown in Figs. 1–3. PCO_2 changes with reference to the steady state P_0 occur as a result of a step input of P_I = 37 mmHg (or F_I = 5%) applied at t = 0, while keeping the ventilation level constant at the equilibrium point.

constant(s) of the system. Only the initial period of about 100 sec is pertinent for examining the stability associated with short-term periodicities of the breathing pattern. During this initial period, M2 and M3 are nearly identical and their transient responses are 25% slower than that of the M1 model.

STABILITY CRITERION

To proceed with a stability analysis, we need to define the controller equation relating ventilation to CO_2 pressure. The alveolar ventilation $\dot{V}_A$ is assumed linearly related to the CO_2 partial pressure, $P_s^* = P_s(t - t_d)$:

$$\dot{V}_A = \begin{cases} GP_s^* - I, & P_s^* > I/G \\ 0, & P_s^* < I/G \end{cases} \tag{18}$$

where G and I are the controller gain and intercept parameters, respectively. The time delay is assumed to be that of the systemic arterial delay, $t_d = t_a$. Substituting Eq. 18 into the plant model, Eq. 17, we find

$$dP_s/dt = F(P_s^*, P_s) + M_s/kV_s \tag{19}$$

where

$$F(P_s^*, P_s) = [GP_s^* - I][P_I - P_s]/\lambda V_s.$$

This nonlinear, differential-difference, first-order equation is the minimal, closed-loop representation of the CO_2 respiratory feedback system. To obtain an explicit stability criterion for this system, we shall linearize Eq. 19 about its steady-state operating point ($P_{so} = P_{so}^*$ and $\dot{V}_{Ao}$). When $dP_s/dt = 0$, Eqs. 17 and 18 yield

$$P_{so} = P_I + \lambda M_s/k\dot{V}_A = P_I + \lambda M_s/k[GP_{so} - I]. \tag{20}$$

By rearranging Eq. 20, we find:

$$P_{so}^2 - [P_I + I/G]P_{so} + [IP_I - \lambda M_s/k]/G = 0. \tag{21}$$

The solution of this quadratic equation gives

$$P_{so} = \{P_I + I/G \pm [(P_I + I/G)^2 - 4(IP_I - \lambda M_s)/k)/G]^{0.5}\}/2.$$

We linearize Eq. 19 about $P_s = P_{so}$ and $P_s^* = P_{so}$:

$$F(P_s^*, P_s) = F(P_{so}, P_{so}) + A_s[P_s - P_{so}] + B_s[P_s^* - P_{so}]$$

where

$$A_s = \partial F(P_{so}, P_{so})/\partial P_s = -[GP_{so} - I]/\lambda V_s = -\dot{V}_{Ao}/\lambda V_s$$

and

$$B_s = \partial F(P_{so}, P_{so})/\partial P_s^* = -G[P_{so} - P_I]/\lambda V_s.$$

These relationships are substituted in Eq. 19 to obtain

$$dP_s/dt = A_s P_s + B_s P_s^*. \tag{22}$$

A system in the form of Eq. 22 was shown to be stable by Hayes *et al.* (12) if it satisfies the following conditions:

S.1 $A_s t_d < 1$
S.2 $A_s < -B_s$
S.3 $-B_s t_d < [(A_s t_d)^2 + \rho_1^2]^{0.5}$

where ρ_1 is the root of $\rho cot\rho = A_s t_d$.

The condition S.1 is always satisfied since

$$A_s t_i = -\dot{V}_{Ao} t_d/\lambda V_s < 0.$$

The condition S.2 also is satisfied since $-B_s$ is proportional to $P_{so} - P_I$, which has positive value as shown by Eq. 20. Finally, for typical physiological values (Table 1), we find $A_s t_d \ll 1$ and $\rho_1 \simeq \pi/2$. This simplifies condition S.3 to

$$-2B_s t_d/\pi < 1.$$

Using this criterion and the definition of B_s, we can characterize stability by a single stability index

$$\text{SI} = 2Gt_d[P_{so} - P_I]/\pi\lambda V_s = \text{UF/SF} < 1 \tag{23}$$

where we have arbitrarily defined an unstable factor

$$\text{UF} = 2Gt_d[P_{so} - P_I]$$

and a stable factor

$$\text{SF} = \pi\lambda V_s.$$

Thus, P_s and (via the controller equation) ventilation $\dot{V}_A$ is stable if SI < 1 or UF < SF; ventilation is unstable if SI > 1 or UF > SF.

SYSTEM ANALYSIS

Having derived an explicit stability criterion based on a linearized first-order system (M1), we can examine how variations of system parameters affect the stability index SI. Typical values of human adult (25) are chosen as a reference (Table 1). Furthermore, by formal model reduction we can evaluate the effective tissue volume

($V_{tis} = V_s$) in terms of its fundamental parameters. Consequently, we can establish a reference value for SI. As shown in Fig. 5, increases in controller gain (G), intercept (I), and delay time (t_d) tend to destabilize ventilation. On the other hand, when inspired CO_2 and effective tissue volume are increased, ventilation tends to be more stable. Metabolic rate has only a small effect on stability. These predictions agree with previously reported experimental, clinical and theoretical results (6,19,20).

To validate the analytical results based on the linearized first-order model, we have to investigate the effect of nonlinearity on the stability criterion. This nonlinearity occurs because of the multiplicative P_s terms and the incorporation of a threshold below which the alveolar ventilation is zero. These effects on the stability can be determined by numerical solution of the nonlinear model M1 (Eq. 19). If the system is perturbed, V_A may oscillate indefinitely (an unstable response) or may return to its base-line value (a stable response). Examples of these responses are given in Fig. 6.

The stability characteristics are presented in terms of the two parameter groups, UF and SF (Fig. 7). This parameter space is divided into stable and unstable domains by the slope SI of the analytical relation, Eq. 23. Also shown are the domains determined by numerical solution of the nonlinear model, Eq. 19, for various combinations of V_s and t_d, which are linearly related to SF and UF, respectively. The numerical solution was classified as stable (for a damped response) or unstable (for sustained oscillation). The simulated value of SI is only 10% greater than that predicted analytically from the linearized model. Because the numerical simulations indi-

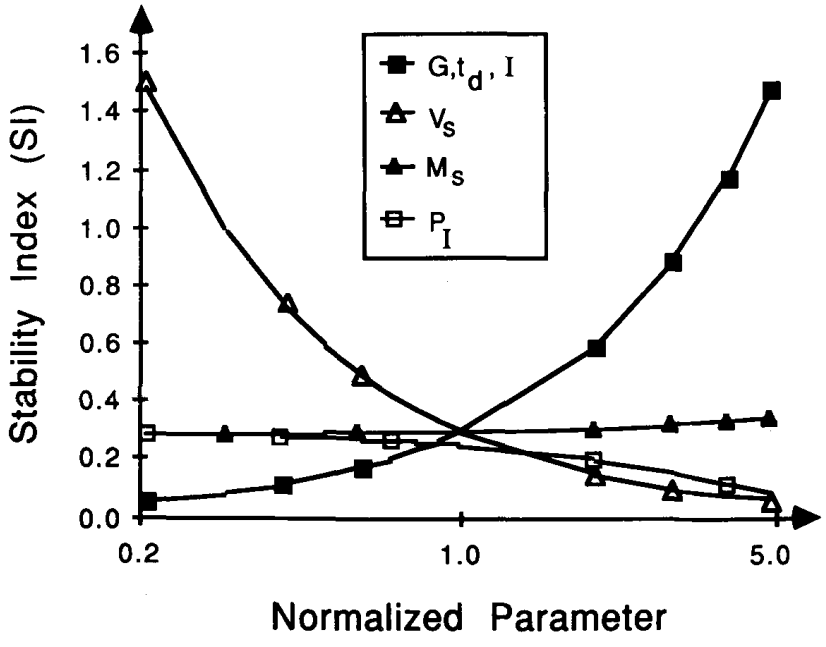

FIGURE 5. The stability index (SI) as a function of various system parameters on a semi-logarithmic scale. The parameters were normalized by their mean typical values as given in Table 1 except for P_I, which is normalized by 8 mmHg. Variations in G were accompanied by proportional changes in I and M_s to keep the operating point constant.

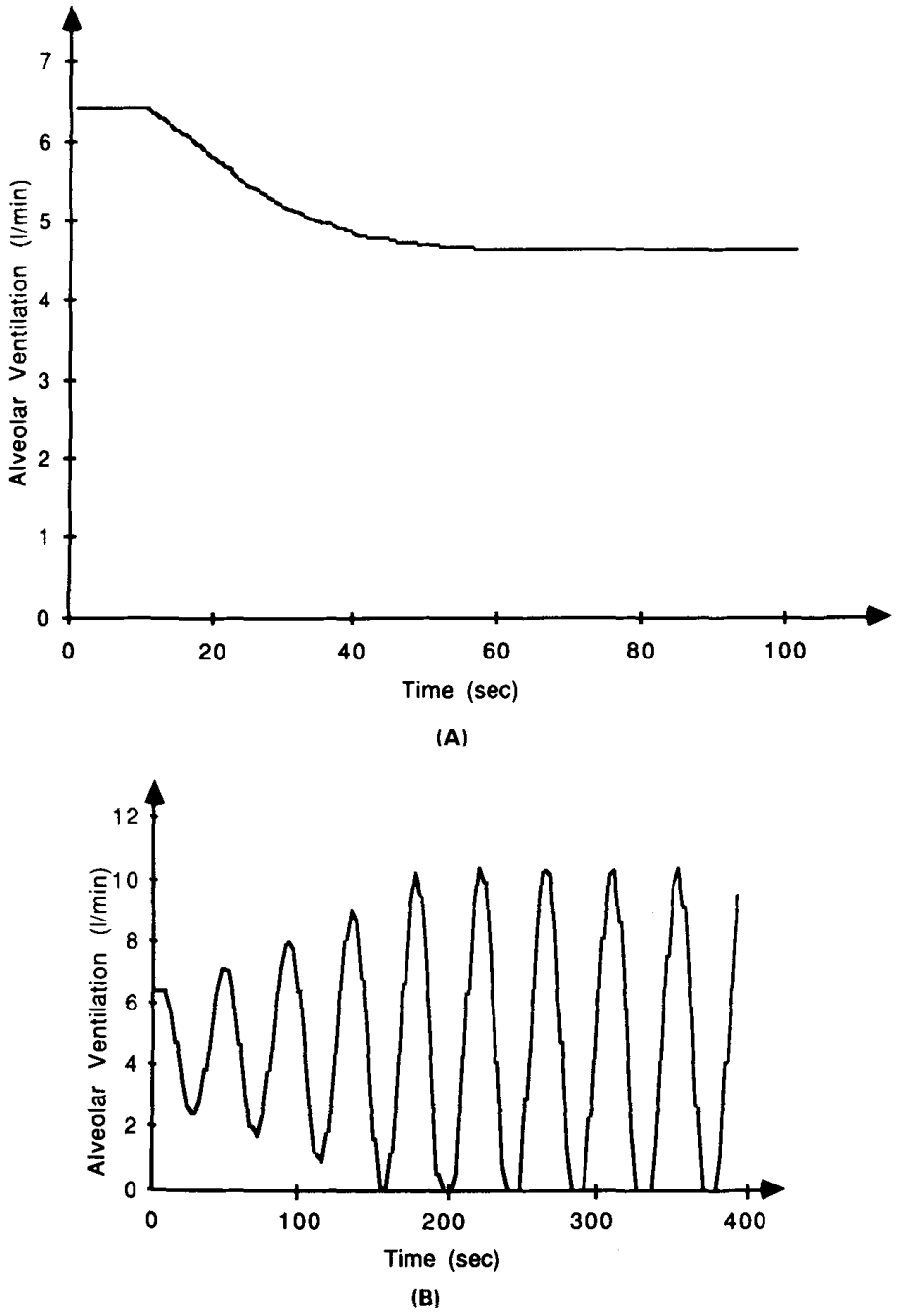

FIGURE 6. Typical patterns of stable (A) and unstable (B) responses. The parameters for the stable case are those listed in Table 1. For the unstable case, V_s was reduced to 2.5 L.

cate that the domain of stability is increased, we modify the stability domain as follows:

$$SI < 1.1. \tag{24}$$

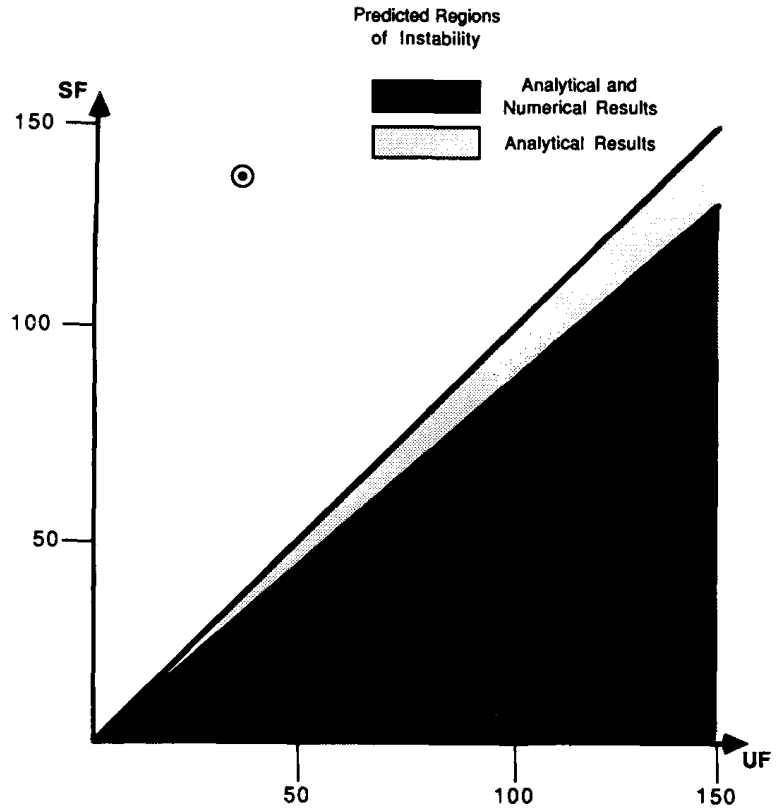

FIGURE 7. Comparison of analytical predictions based on the linearized 1-compartment model and simulations using the nonlinear 1-compartment model. The circled point represents the values for typical parameters as listed in Table 1.

DISCUSSION

The theoretical studies described above proceed in two distinct steps. First, a reduced model of whole-body CO_2 stores was developed from a more general model by formal procedures of model reduction. Second, this plant model was combined with a controller representing peripheral chemoreceptor control of ventilation and a formal analysis of the stability properties of this closed-loop system was performed. It is appropriate to consider first the limitations of these procedures.

This study is concerned with the development of sustained, small-amplitude periodicities (STP) in ventilation. Initiation of such oscillations may result from transient disturbances which elicit responses that are initially independent of certain system properties; but if an oscillation is to be sustained, then CO_2 flux (and not just partial pressures) throughout the body must be considered. Thus, we included all the body stores for CO_2 with the presumption that if the contribution of some compartment were trivial, then this result would naturally be apparent from the formal mathematical reduction of the model.

To apply the Hayes (12) stability criterion, it was necessary to represent the plant as a first-order system. The 3-compartment model of CO_2 stores, in which the brain compartment is included with "other tissue," has been shown by others to be an ade-

quate model of CO_2 plant dynamics. In contrast to other studies, we combined the (nonalveolar) tissue compartments into a single compartment by a "small-time" or perturbation analysis. This leads to a much smaller volume (13.4 L) of the equivalent tissue space than that (38.7 L) obtained by algebraic addition of compartmental volumes (10,19). The value predicted by our analysis is close to the 15 L assumed by other investigators (13,14) to simulate experimentally observed dynamics. By order-of-magnitude approximations, with respect to time delays and time constants, the plant model was reduced to a first-order system. The adequacy of these assumptions was tested by comparing the dynamic response of the first-order plant model to a step change in inspired CO_2 to that of the original 3-compartment plant model. While these responses diverge considerably for times between 1000–3000 seconds, they are comparable on a "small" time scale (20–120 sec) appropriate for investigating STP. The 25% error over the first 100 seconds of the response implies that the reduced model may over-estimate somewhat the tendency for instability.

Based on the results of Khoo *et al.* (13), we assumed that central chemoreceptors did not contribute to oscillations in ventilation occurring during periodic breathing because their effective "loop gain" would be too low at these short periods of oscillation. Therefore, the controller was assumed to sense the plant CO_2 delayed by the lung-to-peripheral chemoreceptor transport time. The resultant model is qualitatively comparable to that used by Khoo *et al.* (13) for determining peripheral CO_2 loop gain and phase shift for use with another stability criterion, namely the Nyquist criterion.

A difficulty arises because the static equilibrium point depends on the total central plus peripheral CO_2 gain, whereas the analysis for STP assumes that the central contribution is negligible. In this preliminary study, we can demonstrate the feasibility of our analysis with a combined value for CO_2 gain (2.33 L/min/Torr). For comparisons with experimental data, the two gains have to be distinguished. In the present case, it can be assumed that the increased peripheral CO_2 sensitivity would relate to a situation of mild hypoxia. Indeed, Berssenbrugge *et al.* (1) have reported that mild hypoxia is necessary for the development of periodic breathing in quiet sleep. The effect of mild hypoxia on the equilibrium point would have only a small quantitative influence on the behavior predicted by our model.

By a rigorous reduction of the plant to a first-order system, we derived a single stability index, SI, as a function of relevant system parameters. Analytical and numerical techniques were applied to obtain and verify that SI determines whether the alveolar ventilation is stable or unstable. Using SI, we can predict ventilation stability in terms of any combination of parameters. This is in contrast to the simulation study by Milhorn *et al.* (19) in which the system behavior was examined by varying one parameter and keeping other parameters constant. Exhaustive simulations of different combinations of all parameter variations would be a formidable task and would not necessarily lead to proper generalizations.

The work of Glass and Mackey (9) and Mackey *et al.* (16,17) uses the same stability technique of Hayes *et al.* (12) that we apply. However, their derived stability criterion is based on an empirical model of CO_2 plant dynamics and the physiological interpretation of the model parameters (corresponding to A_s and B_s in Eq. 22) was not validated. Indeed, this model and the stability criterion imply that an increase in metabolism destabilizes ventilation, which conflicts with the conclusion of Milhorn and Guyton (19) based on simulations with a more physiological model. Further-

more, the *ad hoc* relationships given by Mackey *et al.* (16,17) do not include the effect of inspired CO_2 concentration. In contrast, our approach started with a sufficiently general dynamic CO_2 mass balance and reduced the model in a well-defined and rigorous manner.

The representation of CO_2 and O_2 control of respiration by Khoo *et al.* (13) is more complete than ours, but it has several drawbacks. First, their implicit stability criterion, which is based on the Nyquist method, requires the solution of a transcendental equation. This is in contrast to the single explicit index, SI. Second, the model dynamics were not simulated and compared with analytical and experimental results. Therefore, effects of the model assumptions and linearization were not evaluated.

Several key points are elucidated by our analysis. First, if the controller gain (G) is four times the normal value, then SI > 1.1 and ventilation will be unstable. This demonstrates the importance of controller gain as shown by others (12,19) and lends support to the hypothesis that STP is due to unstable ventilatory response associated with CO_2 feedback control. Second, while CO_2 in inspired gas (P_I) can regularize ventilation (20), our analysis using SI shows that the effectiveness of CO_2 may vary depending on the cause of instability. Third, in contrast to the analyses of other investigators (7), we predict that controller intercept (I) is not a direct critical factor in ventilatory dynamic responses. Rather, it has an indirect effect through the equilibrium point (P_{so}) of the system. For example, sustained oscillations which contain no apneic duration may be obtained by simultaneously increasing the metabolic rate and intercept.

Further analysis of chemical control of respiration will require separating the controller into peripheral and central components and incorporating the effects of O_2 dynamics. Nevertheless, this study provides a valuable paradigm that can lead to better quantitative understanding of the respiratory control system and its stability characteristics.

REFERENCES

1. Berssenbrugge, A.; Dempsey, J.; Iber, C.; Skatrud, J.; Wilson, P. Mechanism of hypoxia-induced periodic breathing during sleep in humans. J. Physiol. 343L 507–524; 1983.
2. Brown, H.W.; Plum, F. The neurologic basis of Cheyne-Stokes respiration. Am. J. Med. 30:849–860; 1961.
3. Cherniack, N.S. Sleep apneas and its causes. J. Clin. Invest. 73:1501–1506; 1984.
4. Cherniack, N.S.; Longobardo, G.S. Cheyne-Stokes breathing: An instability in physiologic control. N. Eng. J. Med. 288:952–957; 1973.
5. Cherniack, N.S.; Longobardo, G.S. Abnormalities in respiratory rhythm. In: Cherniack, N.S.; Widdicombe, J.G., Eds., Handbook of Physiology, Sec. 3, Vol. 2, Part 2. Bethesda, MD: Am. Physiol. Soc.; 1986: pp. 729–749.
6. Cherniack, N.S.; Von Euler, C.; Homma, I.; Kao, F.F. Experimentally induced Cheyne-Stokes breathing. Resp. Physiol. 37:185–200; 1979.
7. Dempsey, J.; Skatrud, J.B. A sleep-induced apneic threshold and its consequences. Am. Rev. Respir. Dis. 133:1163–1170; 1986.
8. Dowell, A.R.; Buckley, E.; Cohen, R.; Whalen, R.E.; Seiker, H.O. Cheyne-Stokes respiration. A review of clinical manifestations and critique of physiological mechanisms. Arch. Int. Med. 127:712–726; 1971.
9. Glass, L.; Mackey, M. Pathological conditions resulting from instabilities in physiological control systems. Ann. N.Y. Acad. Science 316: 214–235; 1979.
10. Grodins, F.S.; Buell, J.; Bart, A.J. Mathematical analysis and digital simulation of the respiratory control system. J. Appl. Physiol. 22:260–276; 1967.

11. Guyton, A.C.; Crowell, J.W.; Moore, J. The basic oscillating mechanism of periodic breathing in cardiac failure. Circulation 12:717; 1956.
12. Hayes, N.D. Roots of the transcendental equation associated with a certain difference-differential equation. J. London Math. Soc. 25:226–232; 1950.
13. Khoo, M.C.K.; Kronauer, R.E.; Strohl, K.; Slutsky, A.S. Factors inducing periodic breathing in humans: A general model. J. Appl. Physiol. 53:644–659; 1982.
14. Longobardo, G.S.; Cherniack, N.S.; Fishman, A.P. Cheyne-Stokes breathing produced by a model of the human respiratory system. J. Appl. Physiol. 21:1839–1846; 1966.
15. Longobardo, G.S.; Gothe, B.; Goldman, M.D.; Cherniack, N.S. Sleep apnea considered as a control system instability. Resp. Physiol. 50:311–333; 1982.
16. Mackey, M.; Glass, L. Oscillation and chaos in physiological control systems. Science 197:287–289; 1977.
17. Mackey, M.; Heiden, U.A.D. Dynamical diseases and bifurcations: Understanding functional disorders in physiological systems. Funk. Biol. Med. 1:156–164; 1982.
18. Matthews, C.M.E.; Laszlo, G.; Campbell, E.J.M.; Read, D.J.C. A model for the distribution of CO_2 in the body and the ventilatory response to CO_2. Resp. Physiol. 6:45–87; 1969.
19. Milhorn, H.T. Jr.; Guyton, A.C. An analog computer analysis of Cheyne-Stokes breathing. J. Appl. Physiol. 20:328–333; 1965.
20. Pembery, M.S.; Allen, R.W. Observations upon Cheyne-Stokes respiration. J. Physiol. 32: XVIII–XX; 1905.
21. Plum, F.; Brown, H. Neurogenic factors in periodic breathing. Trans. Amer. Neurological Association, 86:39–42; 1961.
22. Preiss, G.; Iscoe, S.; Polosa, C. Analysis of a periodic breathing pattern associated with Mayer waves. Am. J. Physiol. 228:768–774; 1975.
23. Pryor, W.W. Cheyne-Stokes respiration in patients with cardiac enlargement and prolonged circulation-time. Circulation 4:233; 1951.
24. Remmers, J.E.; de Groot, J.W.; Sauerland, E.K.; Anch, A.M. Pathogeneses of upper airway occlusion during sleep. J. Appl. Physiol. 44:931–938; 1978.
25. Saunders, K.B.; Bali, H.N.; Carson, E.P. A breathing model of the respiratory system: The controlled system. J. Theor. Biol. 84:135–161; 1980.
26. Youmans, W.B.; Schopp, R.T. Cheyne-Stokes breathing after denervation of carotid and aortic chemoreceptors and sino-aortic pressoreceptors. Proc. Soc. Exptl. Biol. Med. 95:100–101; 1957.

APPENDIX

CO_2 Mass Balance Equations

The general model that serves as the basis for our analysis consists of four perfectly mixed compartments: alveolar gas (AG), alveolar tissue (at), muscle tissue (mt), and other (nonmuscle) tissue (ot) as shown in Fig. 1. We shall derive the CO_2 dynamic mass balances for each of these compartments and then express these balance equations in terms of CO_2 partial pressures. In the alveolar gas space, the concentration (moles/liter) of CO_2 (C_{AG}) changes through alveolar ventilation ($\dot{V}_A$) and by the diffusion rate (D) between alveolar gas and tissue. Averaging over the breathing cycle, we obtain the molar rate of CO_2 change:

$$V_{AG}dC_{AG}/dt = D + \dot{V}_A[C_I - C_{AG}]. \tag{A.1}$$

In this breath-averaged analysis, the alveolar gas volume (V_{AG}) and inspired CO_2 concentration (C_I) are assumed constant.

The total molar concentration of CO_2 in the alveolar tissue (C_{at}) depends on the blood flow (Q) and diffusion rate (D):

$$V_{at}dC_{at}/dt = -D + Q[C_v(t - t_v) - C_a] \tag{A.2}$$

where V_{at} is the composite volume of tissue including the blood. The mixed venous blood CO_2 concentration $C_v(t - t_v)$ entering the alveolar tissue is delayed by t_v from the venous concentration leaving the systemic tissues. As the blood output of the alveolar tissue, we have the arterial blood concentration C_a.

Let us consider the diffusion rate between alveolar gas and tissue to be

$$D = \alpha[C_{at} - \sigma C_{AG}] \tag{A.3}$$

where α is a rate coefficient for mass transfer and λ is a tissue (blood)-gas partition coefficient. When α is sufficiently large, CO_2 equilibrium between the tissue and gas is approached:

$$C_{at} \simeq \sigma C_{AG}. \tag{A.4}$$

Consequently, (A.1) and (A.2) are not independent equations. We can sum these equations using (A.4) and the following definitions

$$C_A = C_{AG}, \qquad C_a = C_{at}, \qquad C_v^* = C_v(t - t_v), \qquad V_A = V_{AG} + \sigma V_{at}$$

to obtain

$$V_A dC_A/dt = \dot{V}_A[C_I - C_A] + Q[C_v^* - C_a]. \tag{A.5}$$

To express this in terms of CO_2 partial pressures, we use the ideal gas relations for $x = A, I$:

$$C_x = P_x/RT. \tag{A.6}$$

Also, we assume that the CO_2 equilibrium relation between total and free CO_2 has the same linear form in all tissues:

$$\Delta C = k\Delta P \tag{A.7}$$

which implies

$$C_v^* - C_a = k[P_v^* - P_a].$$

Consequently, inserting (A.6) and (A.7) into (A.5) yields

$$V_A dP_A/dt = \dot{V}_A[P_I - P_A] + \lambda Q[P_v^* - P_a] \tag{A.8}$$

where $\lambda = kRT$.

Next, we shall consider the systemic tissues which differ with respect to perfusion and metabolism. In the resting state, one can distinguish between poorly perfused muscle tissue (m) and well-perfused other tissues (ot). For the muscle tissue compartment, the CO_2 (molar) concentration (C_m) depends upon the rate of metabolism (M_m) as well as the blood flow (Q_m):

$$V_m dC_m/dt = M_m + Q_m[C_a^* - C_m] \tag{A.9}$$

where the arterial CO_2 concentration input $C_a^* = C_a(t - t_a)$ is delayed by t_a with respect to the arterial blood CO_2 concentration leaving the alveolar tissue. A similar balance describes the CO_2 molar concentration of other tissues (C_{ot}):

$$V_{ot}dC_{ot}/dt = M_{ot} + Q_{ot}[C_a^* - C_{ot}]. \tag{A.10}$$

Using the equilibrium relation (A.7), we can express the CO_2 tissue dynamics of Eqs. (A.9) and (A.10) as

$$V_m dP_m/dt = M_m/k + Q_m[P_a^* - P_m] \tag{A.11}$$

and

$$V_{ot}dP_{ot}/dt = M_{ot}/k + Q_{ot}[P_a^* - P_{ot}]. \tag{A.12}$$